Scientific Journals
of the Maritime University of Szczecin

Zeszyty Naukowe
Politechniki Morskiej w Szczecinie

2024, 80 (152), 23–31
ISSN 2392-0378 (Online)
DOI: 10.17402/621

Received: 30.06.2024
Accepted: 26.11.2024
Published: 31.12.2024

Effect of mesh density and grid type on cavitation cloud volume

Robert Jasionowski[1], Waldemar Kostrzewa[2]

[1] https://orcid.org/0000-0002-2943-3593

Maritime University of Szczecin, Department of Machine Construction and Materials
2-4 Willowa St., 71-650 Szczecin, Poland
e-mail: [1]r.jasionowski@pm.szczecin.pl, [2]w.kostrzewa@pm.szczecin.pl
corresponding author

Keywords: computational fluid dynamics (CFD), CFD simulation, meshing, multiphase flow models, cavitation, cavitation model, cavitation cloud, cavitation tunnel

JEL Classification: C38, C63, C88, L95

Abstract

This work is devoted to determining the effect of mesh density and mesh type on cavitation cloud volume generated during the flow of water through the cavitation tunnel. The numerical analysis was carried out on a water model based on a cavitation tunnel located at the Institute of Water Problems of the Bulgarian Academy of Sciences in Sofia, used to test the resistance of construction materials to cavitation erosion. A numerical analysis is performed for four different types of grids: polyhedra, poly-hexcore, hexcore, and tetrahedral. These grids have five different maximum cell sizes: 0.0025, 0.0020, 0.0015, 0.0010, and 0.0005 m. A numerical analysis is performed using commercial CFD software – i.e., Ansys Fluent 2023 R1. The Schnerr and Sauer cavitation model and the k-omega viscous model for shear stress transport (SST) are used. This paper analyzes the qualitative parameters of the quality of the grid, distribution of velocity, pressure, average cell volume, and volume of cavitation cloud consisting of 90% volume vapor fraction. Based on the numerical analyses, it is shown that the basis for obtaining accurate results of the CFD simulations is not only the qualitative parameters of the grid but also its density.

Introduction

Cavitation is the process of formation of vapor bubbles that grow and then collapse as the pressure recovers above vapor pressure, causing implosion (Plesset, 1949; Plesset & Chapman, 1971; Brennen, 1995; Young, 1999; Franc & Michel, 2004). The implosion of cavitation is an effect of pressure change from the area of its low value to a region of elevated pressure, causing condensation of steam that fills the cavitation bubble. The implosion phenomenon occurs at very high velocity (exceeding 100 m/s), and, in such a case, the time of growth and decay of a cavitation bubble is in the order of milliseconds. A cavitation is a form of wear that commonly damages propellers, turbine blades, valve seats, or any material in proximity to collapsing bubbles. Undesirable effects of cavitation are mainly erosion, noise, and loss of performance in flow machines (pumps, water turbomachinery, and others) (Liu et al., 2014; Muttalli, Agrawal & Warudkar, 2014; Szala & Łukasik, 2016; Sánchez Ocaña et al., 2018; Hu, Yang & Cao, 2020; Hu, Yang & Shi, 2020). Cavitation is prevented by using more resistant materials (often by changing the properties and structure of the material itself), adding inhibitors to the liquid and changing the design of machinery and flow equipment (Zasada, Sienkiewicz & Jasionowski, 2015; Jasionowski, Polkowski & Zasada, 2018; Lin et al., 2018; Zakrzewska & Krella, 2019). In recent years, an increasingly popular method of understanding the phenomenon of cavitation

and its occurrence is the use of computational fluid dynamics (CFD) (Jasionowski & Kostrzewa, 2018, 2023; Johnsen & Colonius, 2009; Müller, Helluy & Ballmann, 2010; Lauer et al., 2012).

For numerical simulations of cloud cavitation, the Eulerian-Lagrangian approach is most commonly used, in which the pressure field is used to calculate the dynamics of the bubbles. The Eulerian–Lagrangian method combines the averaging approach and the Lagrangian approach; it solves the dynamics of the mixture on an Eulerian grid, while tracking the dynamics of Lagrangian point bubbles at the subgrid scale. The Eulerian–Lagrangian method is free from the spatial limitation in the averaging approaches as well as from the constraint on the wavelength of the far-field pressure in the Lagrangian point-bubble approaches. Accurate simulations of cloud cavitation are in high demand for such applications, yet they are challenging due to the complex, multiscale nature of the interactions among the dynamics of small, dispersed bubbles and pressure waves propagating in the liquid (Naudé & Ellis, 1961; Rasthofer et al., 2017; Tiwari, Pantano & Freund, 2015).

A very important step in the process of analyzing and simulating CFDs is generating a grid. The production of a high-quality mesh is extremely important to obtain the correct solutions and guarantee the stability of the numerical analysis. Grid generation is a very difficult process in which decisions have to be made on the arrangement of discrete points (nodes) throughout the computational domain and the type of connections for each point. The quality of the grid very often leads to the success or failure of numerical simulation. Improving the resolution of a compute grid by reducing or increasing the size of the grid cells leads to more accurate simulation results at the expense of the time needed to perform the calculations (Thompson, Warsi & Mastin, 1985; Peyret, 1996; Liseikin, 1999).

CFD simulations are performed for two different models: 2D and 3D. For 2D models, cells with regular shapes are most commonly used, while for 3D models with complex geometry, grids with irregular shapes of cells are used. Four types of volume mesh are most commonly used for creating 3D models (Ansys, 2024):

- *Polyhedral* meshes have more neighboring cells compared with tetrahedral cells and, thus, more easily capture gradients with far fewer cells (recommended for recirculating flows).
- *Poly-hexcore* meshes fill the bulk region with octree hexes, keeping a high-quality layered polyprism mesh in the boundary layer and conformally connecting these two meshes with general polyhedral elements.
- *Hexcore* meshing is a hybrid meshing scheme that generates Cartesian cells inside the model and tetrahedral cells close to the boundaries. Hexcore meshing has fewer cells and is fully automated, which is used to handle complex geometries, internal walls, and gaps. The hexcore meshing scheme is applicable to all volumes but is mainly useful for volumes with large internal regions and few internal boundaries, such as intrusions or holes.
- *Tetrahedral* meshes lend themselves to automatic meshing of very complex fluid volumes, however, at the expense of very high cell counts (typically 3–4 times higher).

Obtaining correct results using the numerical CFD simulation depends on the type of grid used for the analysis and its density. The quality of the grid can be verified using the following parameters (Ansys, 2024):

- **Aspect ratio calculation for triangles**. The aspect ratio of a triangle provides a comparison of the "height" and "width" of a triangle.
- **Aspect ratio calculation for quadrilaterals**. The aspect ratio of quadrilaterals provides a comparison of a long side to a short side of the quadrilateral.
- **Jacobian ratio**. The Jacobian ratio is a measurement of the shape of a given element compared with that of an ideal element. The ideal shape of an element depends on the element type.
- **Warping factor**. The warping factor is computed and tested for some quadrilateral shell elements, as well as the quadrilateral faces of bricks, wedges, and pyramids.
- **Parallel deviation**. Parallel deviation is a measure of how much two parallel sides of a shape deviate.
- **Maximum corner angle**. This is the maximum angle between adjacent edges of an element. For a triangle, the best maximum angle is 60 degrees. For a quadrilateral, it is 90 degrees.
- **Skewness**. Skewness is one of the primary quality measures for a mesh. Skewness determines how close to ideal (equilateral or equiangular) a face or cell is.
- **Orthogonal quality**. The range for orthogonal quality is 0–1, where a value of 0 is worst, and a value of 1 is best.

Note that the quality of the grid is based on the ratio of the volume to the sum of the square of the edge lengths for 2D quad/tri elements, or

the square root of the cube of the sum of the square of the edge lengths for 3D elements.

This paper describes the effect of mesh density and type on the volume of the cavitation cloud generated during the flow of liquid in the cavitation tunnel. The main objective of this research is to determine the influence of the mesh type and its density on the parameters of liquid flow and the formation of the cavitation cloud. Taking into account the quality indicators of the grid, the accuracy of the results of the flow simulation, and the volume of the cavitation cloud, it is possible to determine the optimal parameters of the numerical analysis. The optimal selection of grid parameters allows us to fully utilize the potential of the software to obtain accurate and reliable results as well as to shorten the simulation time.

Numerical model

The geometric model of a cavitation tunnel

A numerical analysis was carried out for a model of the geometric cavitation tunnel located at the Institute of Water Problems of the Bulgarian Academy of Sciences in Sofia (Steller & Gireń, 2015). The numerical simulations were executed using Ansys Fluent 2023 R1. The cavitation tunnel located in the Institute of Water Problems is used to test the resistance to cavitational erosion of different materials. The model of the cavitation tunnel, with a flow area of 0.0002 m^2 (i.e., a width of 0.040 m and a height of 0.005 m) and a length of 0.260 m with a cylindrical cavitator with a diameter of 0.020 m placed at a distance of 0.090 m from the entrance to the tunnel, is shown in Figure 1.

Mesh model

In this paper, the numerical simulations for the cavitation tunnel were executed using the commercial CFD software – Ansys Fluent 2023 R1. The four types of meshing available in Ansys Fluent 2023 R1 were used for the simulation: polyhedral, poly-hexcore, hexcore, and tetrahedral. These are limited by the maximum size of a single cell in terms of five variants: 0.0025, 0.0020, 0.0015, 0.0010, and 0.0005 m. The volume mesh models with the 0.0025-m mesh variant are presented in Figure 2, while the exact geometric parameters of the mesh are presented in Table 1.

The generated grids in Ansys Fluent 2023 R1, having five variants in terms of cell size, were checked

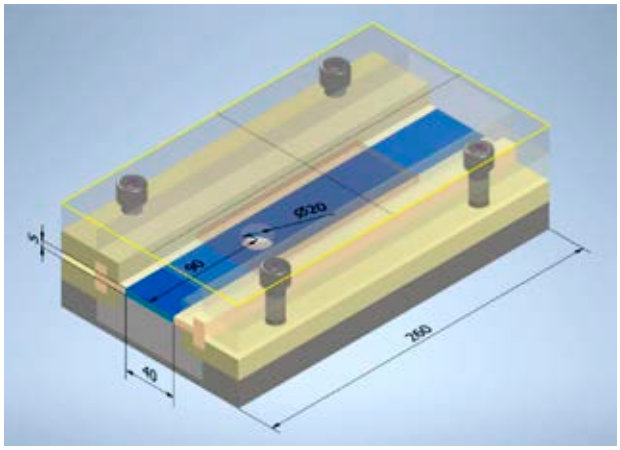

Figure 1. Model of the geometric cavitation tunnel

for quality by three basic parameters: orthogonal quality, aspect ratio, and skewness. The orthogonal quality parameter is calculated for cells using a normal vector to the cell surface, a vector from the center of gravity of the cell facing the center of gravity of the neighboring cell, and a vector from the center of gravity of the cell facing the center of the wall. The orthogonal quality parameter for all mesh types is shown in Figure 3.

The best orthogonal quality parameter was achieved by a polyhedral and poly-hexcore mesh; the worst by a hexcore mesh. The orthogonal quality for the tetra mesh was at a constant level. The parameter difference between the least and most compacted mesh was only 2%.

The aspect ratio parameter is defined as the ratio of the longest side of the figure to the shortest side of the figure. The value of the shape parameter starts with the value of 1, corresponding to the ideal geometry. The lower the aspect ratio parameter value (a value of 1 is best), the higher the mesh quality. The aspect ratio parameter is shown in Figure 4.

All types of meshes have a very low aspect ratio parameter since, for all the variants tested, it is less than 10. The best parameter is shown by two meshes: hexcore and tetrahedral. In Ansys Fluent 2023 R1, skewness typically refers to the skewness of elements in a finite element mesh. Skewness is a measure of how distorted or non-ideal the shape of an element is in a mesh. When performing numerical simulations, a grid with high skewness can lead to inaccurate numerical results and convergence problems. Ideally, grid elements should be as close as possible to regular shapes (e.g., triangles, quadrangles, quadrangles, and cubes) to ensure accurate results. For high-quality 3D grids, the skewness parameter should be 0.4. The skewness parameter for all mesh types is shown in Figure 5.

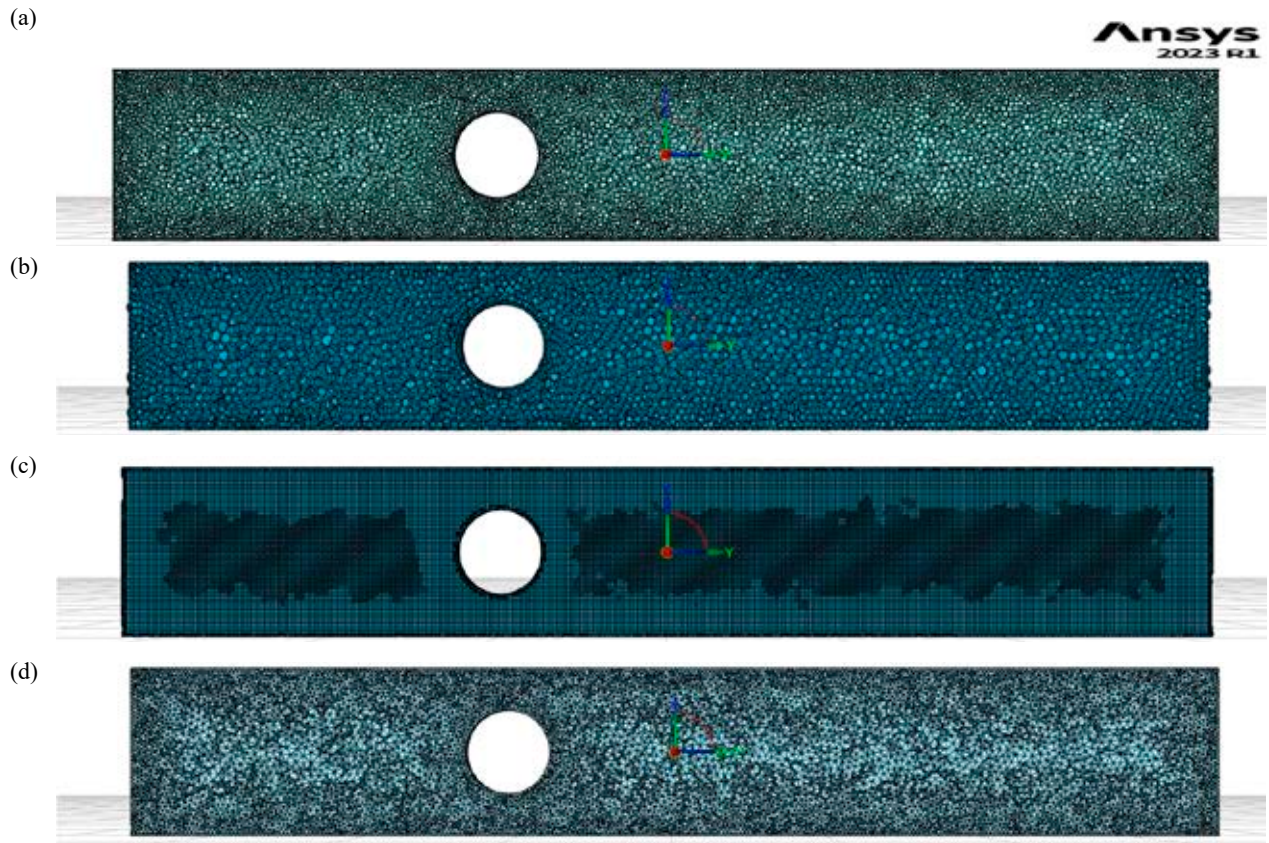

Figure 2. Mesh types with a cell size of 0.0025 m: (a) polyhedral, (b) poly-hexcore, (c) hexcore, and (d) tetrahedral

Table 1. Geometric parameters of the mesh model

Max. cel size [m]	Polyhedral meshing			Poly-hexcore meshing			Hexcore meshing			Tetrahedral meshing		
	Cells	Nodes	Faces	Cells	Nodes	Faces	Cells	Nodes	Faces	Cells	Nodes	Faces
0.0025	45856	263674	299597	13035	76024	82613	258109	93190	598902	217979	46826	453643
0.0020	59626	342182	391991	14294	83225	90657	251827	96209	591787	289778	60298	600178
0.0015	82277	471234	544129	23364	135530	149622	240872	99777	576930	399926	80766	824583
0.0010	181431	1034115	1211061	61655	355551	400067	248375	106084	599950	910272	175616	1863543
0.0005	1517165	8648665	10289277	989822	3545076	5091880	1425547	804863	3642929	6467184	1170104	13103790

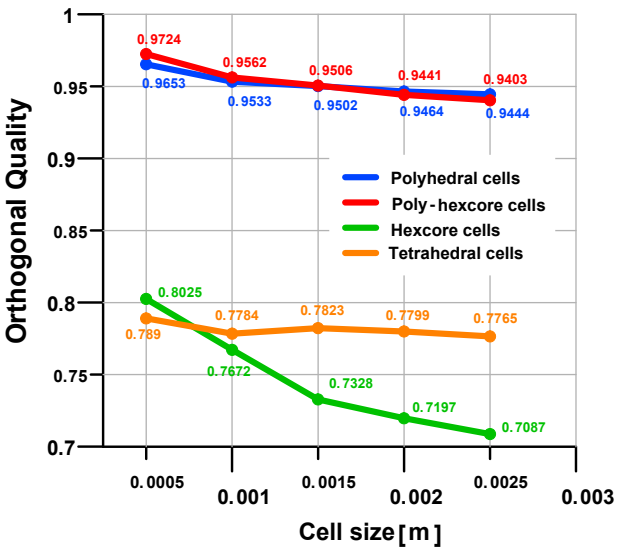

Figure 3. Orthogonal quality parameter for all mesh types

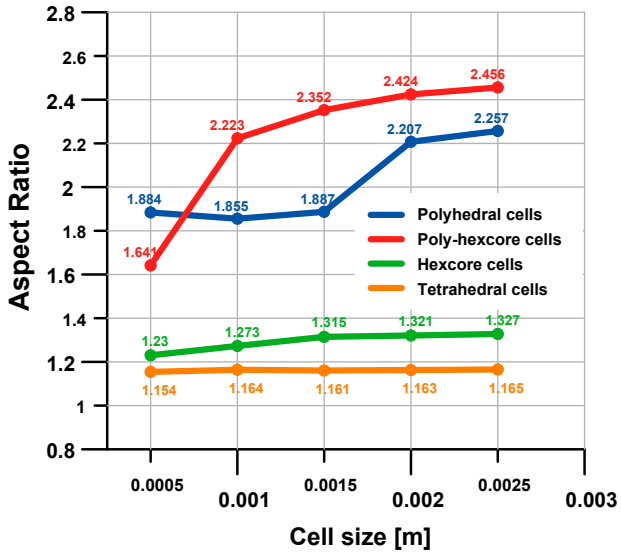

Figure 4. Aspect ratio parameter for all mesh types

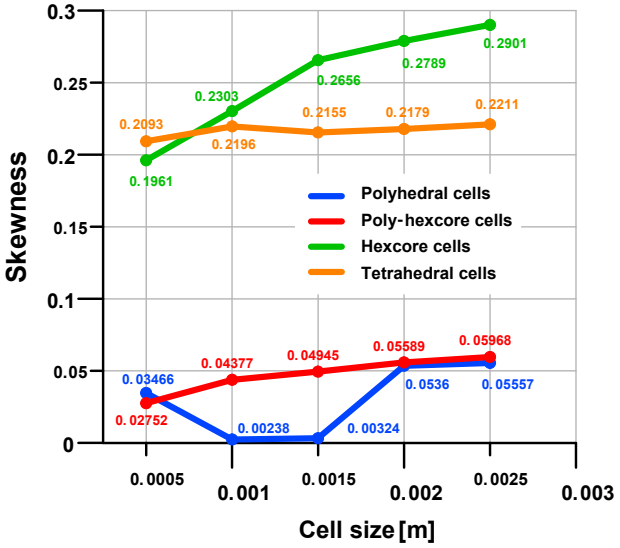

Figure 5. Skewness parameter for all mesh types

All generated types of meshes are characterized by high mesh quality. A perfect mesh quality has polyhedral cells and poly-hexcore cells.

Boundary conditions

The numerical analysis was carried out using a liquid temperature of 16 °C, and the velocity in the tunnel inlet was employed at 22.5 m/s. The following physical parameters were used for water: a density of 0.99894 g/cm^3 and a viscosity of 1108.1 µPa·s. For vapor: a density of 0.5542 g/cm^3 and a viscosity of 13.4 µPa·s.

Cavitation model and solver setup

Multiphase analysis of Schnerr and Sauer cavitation model and transport of shear stress (SST) viscous model k-omega were used for numerical simulation. The coupled algorithm was employed for the pressure-velocity coupling with the PRESTO! discretization scheme applied for the pressure (Ansys, 2024). The quadratic upwind interpolation for the convection kinematics (first-order upwind) scheme was used to discretize the transport equation for the volume fraction of vapor. The details of the models and schemes used in the multiphase cavitating system are given in Table 2. The numerical analysis for each tested variant involved 500 iterations.

Numerical results and analysis

In order to verify the correctness and accuracy of the numerical analyses, the distribution

Table 2. Simulation parameters

Name	Model / Scheme name
Multiphase Flow	Mixture
Cavitation Model	Schnerr-Sauer
Viscous Model	k-omega
k-omega Model	Shear Stress Transport (SST)
Pressure – Velocity Coupling	Coupled Scheme
Spatial Discretization – Gradient	Least Squares Cell-Based
Spatial Discretization – Pressure	PRESTO!
Spatial Discretization – Momentum	First Order Upwind
Spatial Discretization – Volume Fraction	First Order Upwind
Spatial Discretization – Turbulent Kinetic Energy	First Order Upwind
Spatial Discretization – Specific Dissemination Rate	First Order Upwind

of the velocity and pressure of the water flowing through the cavitation tunnel was compared for all tested variants with special consideration of the local extremum for velocity and pressure. The velocity distribution and pressure distribution in the cavitation tunnel for polyhedral mesh with cell size 0.025 m are shown in Figure 6.

Figures 7 and 8 show a comparison of the extreme values of velocity and pressure for all types of grids with different densities.

Analyzing the comparison of extreme local velocity and extreme local pressure values for different types of meshes with different maximum cell sizes, as shown in Figures 7 and 8, we find that the difference in velocity and pressure values between the lowest and highest mesh densities is about 1%. This result clearly shows that the obtained simulation values are correct for each tested variant and that the generated grids are of high quality. In Figures 8 and 9, it can be seen that, with a higher density of the water model mesh (cells size 0.005 m and 0.0010 m), there are increased extreme local values of flow and pressure for each variant analyzed.

The next stage of this research was to determine the average cell volume. Using Ansys Fluent 2023 R1, the average volume of a single cell in all the studied meshes was calculated. The distribution of cell volume for a polyhedral mesh with a cell size of 0.0025 m is shown in Figure 9. The smallest cell volumes were located at the edges of the polyhedral mesh, which results from the assumptions in the generation of the grid. On the basis of cell volume distribution for each analyzed mesh variant,

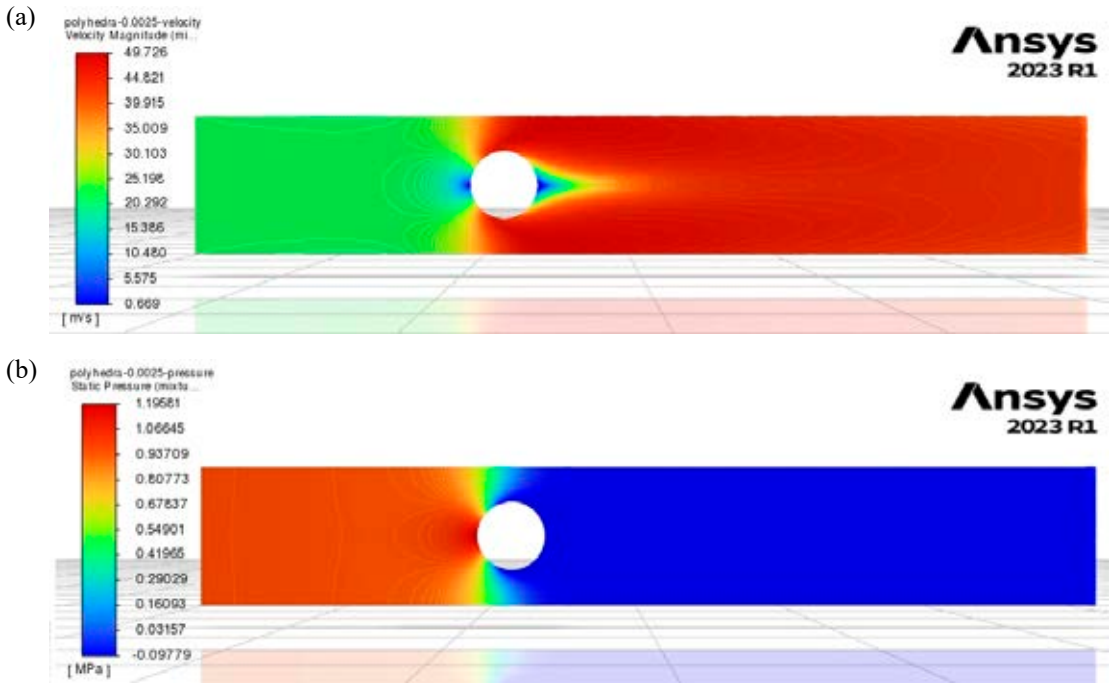

Figure 6. Polyhedral mesh with a cell size of 0.025 m: (a) velocity distribution and (b) pressure distribution

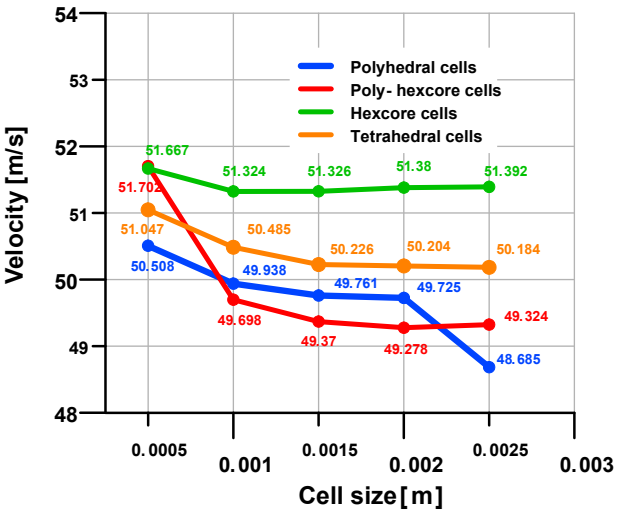

Figure 7. Comparison of the extreme values of velocity for all types of meshes

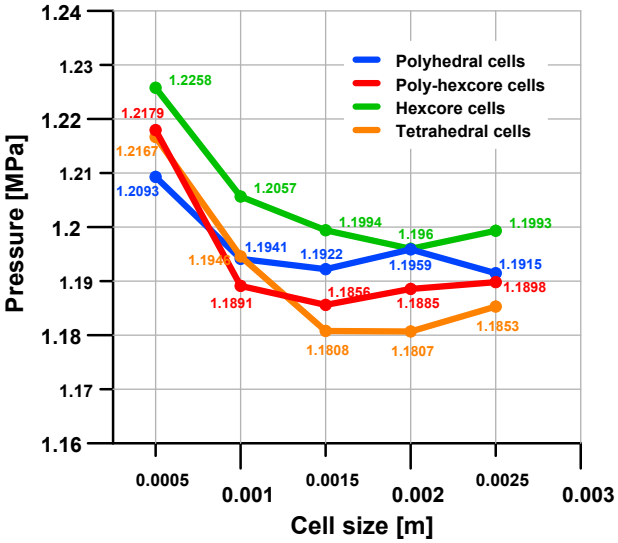

Figure 8. Comparison of the extreme local values of pressure for all types of meshes

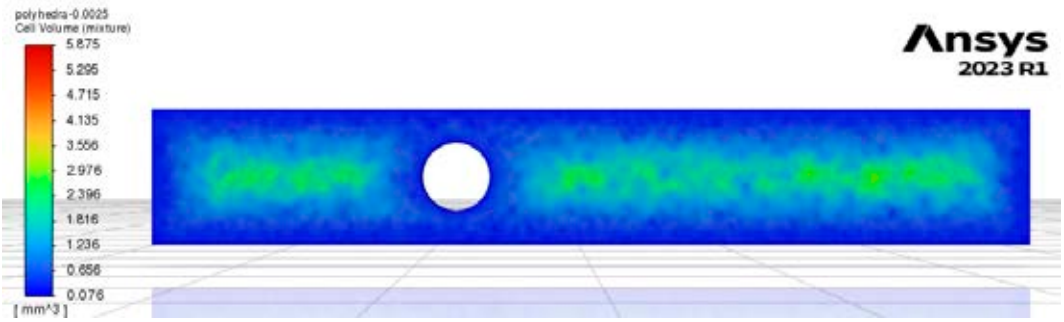

Figure 9. Cell volume for polyhedral mesh with a cell size of 0.0025 m

the average cell volume was calculated. A graph for the average cell volume depending on the type and density of the meshes is shown in Figure 10.

Analyzing the average cell volume graph (Figure 10), it can be seen that poly-hexcore meshes have the highest values. This is due to its polyhedral (multi-walled) type. Polyhedral mesh types are characterized by fewer cells but with greater cell volume. As the cell size decreases, the average cell volume also decreases. For a cell size of 0.0005 m, all the average cell volumes for each analyzed mesh variant are close to each other.

The next stage of this research was to determine the volume vapor fraction. The latter is a cavitation cloud, an area of highly developed cavitation resulting from the geometry of the cavitation tunnel, velocity, and physical properties of the liquid. A cavitation cloud is an area filled with a vapor-gas mixture or cavitation bubbles filled with gas. The volume vapor fraction (cavitation cloud) for polyhedral mesh with a cell size of 0.0025 m is shown in Figure 11.

Considering the volume vapor fraction and, thus, the number of cavitation bubbles forming in the cavitation cloud, the next analysis was carried out for more than 90% of the volume vapor fraction. The cavitation cloud for a volume vapor fraction greater than 90% for a polyhedral mesh with a cell size of 0.0025 m is shown in Figure 12.

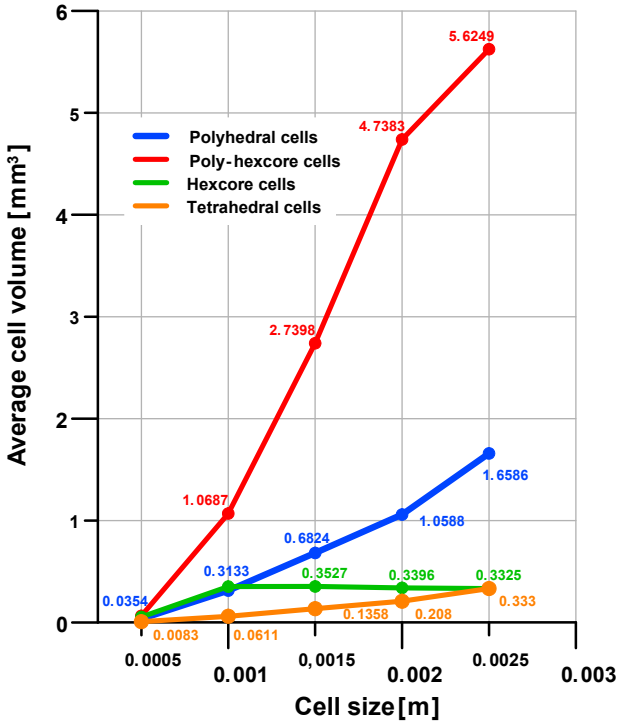

Figure 10. Comparison of the changes in average cell volume depending on the type of mesh

A comparison of the volume of the cavitation cloud calculated from more than 90% of the volume vapor fraction for all the analyzed mesh variants is shown in Figure 13.

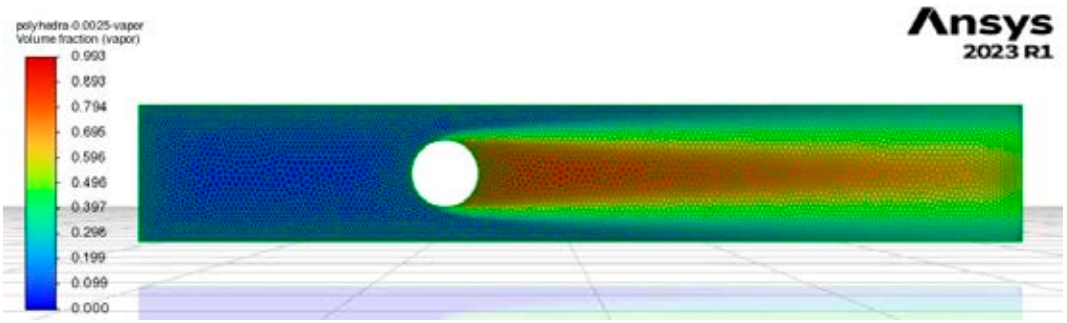

Figure 11. Volume vapor fraction (cavitation cloud) for a polyhedral mesh with a cell size of 0.0025 m

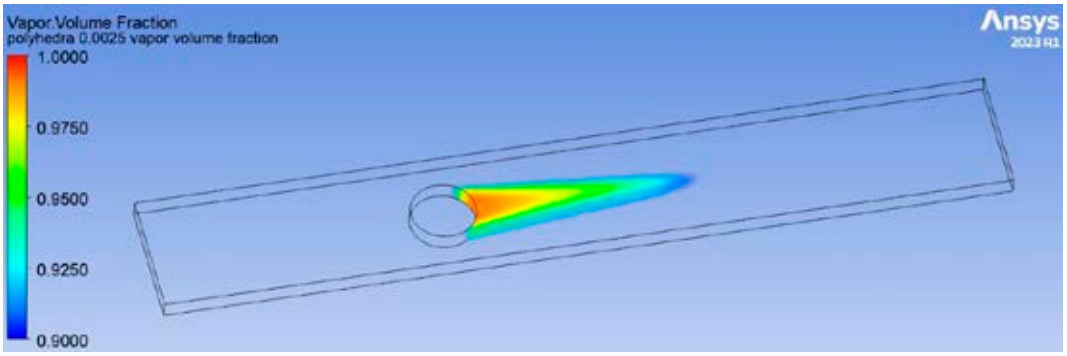

Figure 12. Volume vapor fraction above 90% vapor for a polyhedral mesh with a cell size of 0.0025 m

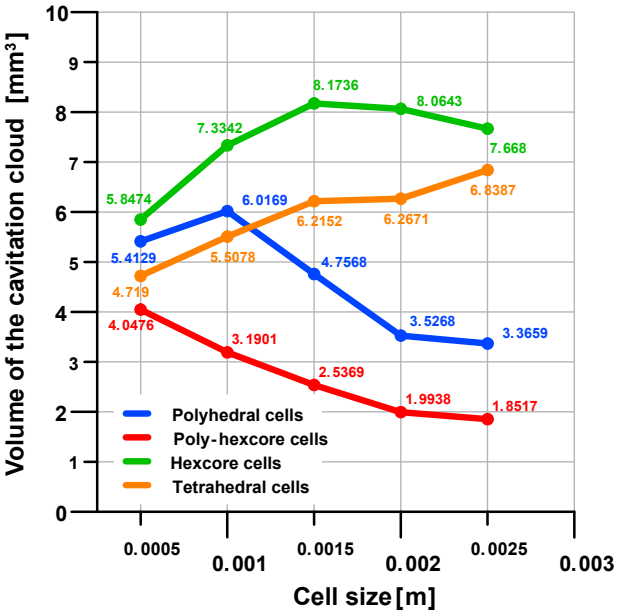

Figure 13. Comparison of the volume of the cavitation cloud calculated from more than 90% of the volume vapor fraction

The volumes of a cavitation cloud consisting of 90% volume vapor fraction for each analyzed mesh variant have different values. The changes in the volumes of a cavitation cloud are directly related to the number of cells and their maximum size and average cell volume. For polyhedral meshes and poly-hexcore meshes, it can be seen that, with a greater density for the mesh, the volume of the cavitation cloud increases. Different waveforms have curves representing hexcore meshes and tetrahedral meshes. For these meshes, an increased mesh density did not cause very large changes in the average cell volume of a single cell. The volume of the cavitation cloud for hexcore meshes increases to a maximum cell size of 0.0015 m, then decreases. For tetrahedral meshes, the volume of the cavitation cloud decreases continuously as the mesh density increases.

Conclusions

ANSYS software has various tools for discretization of the computing domain (universal and simple to use but also more specialized and dedicated to specific applications), as well as a special tool, which is ANSYS Meshing. The discretization of the model is often considered one of the most important elements of computer simulations, whether we want to analyze the flow of air, exhaust, or water. A properly prepared numerical grid is the basis for well-made and reliable calculations. However, this is not an easy task, given that a smaller grid provides better results, but the calculation time is much longer and, therefore, it is necessary to find a balance between accuracy and calculation time. In some cases, the calculation time may be extended many times to improve the accuracy of the results by only 1%.

In the case of the analyzed water model, based on a cavitation tunnel located at the Institute of Water Problems of the Bulgarian Academy of Sciences in Sofia, the following conclusions can be drawn:

- Analyzing the flow parameters, which are the velocity and pressure in the tunnel where the optimal cell size is 0. 0005 m, the difference between the minimum and maximum values of local extremes for the four types of grids is about 2%.
- When analyzing the average cell volumes, the optimal cell size is also 0.0005 m, where all the average cell volumes for each analyzed mesh variant are close to each other.
- Analyzing the volume of the cavitation cloud calculated from more than 90% of the volume vapor fraction, it can be seen that only an additional mesh density of the grid could cause the difference in the obtained results to be smaller. It should be taken into account that the cloud object being analyzed is 90% of the volume vapor fraction, so the differences can be significant given a different type of grid. In addition, it should be remembered that a density of the grid that is too high very often causes the following message to appear during the simulation: “stabilizing pressure coupled to enhance linear solver robustness.” The numerical simulation is then interrupted.

Acknowledgments

Scientific work funded by the Ministry of Science and Higher Education (MEiN) of Poland No. 1/S/KPBMiM/24.

References

1. Ansys (2024) *Ansys Fluent User’s Guide Release 2024 R1*. Ansys Inc., Canonsburg, USA.
2. Brennen, C.E. (1995) *Cavitation and Bubble Dynamics*. Oxford University Press, Oxford, New York.
3. Franc, J.P. & Michel, J.M. (2004) *Fundamentals of Cavitation*. Kluwer Academic Publishers, Kluwer.
4. Hu, Q., Yang, Y. & Cao, W. (2020) Computational analysis of cavitation at the tongue of the volute of a centrifugal pump at overload conditions. *Advances in Production Engineering & Management* 15 (3), pp. 295–306, doi: 10.14743/apem2020.3.366.

5. Hu, Q.X., Yang, Y. & Shi, W.D. (2020) Cavitation simulation of a centrifugal pump with different inlet attack angles. *International Journal of Simulation Modelling* 19 (2), pp. 279–290, doi: 10.2507/IJSIMM19-2-516.
6. Jasionowski, R. & Kostrzewa, W. (2018) Optimization of geometry of cavitational tunnel using CFD method. In: Awrejcewicz, J. (ed.) *Dynamical Systems in Applications*. DSTA 2017. Springer Proceedings in Mathematics & Statistics, vol 249, Springer, Cham, pp. 181–192, doi: 10.1007/978-3-319-96601-4_17.
7. Jasionowski, R. & Kostrzewa, W. (2023) Numerical analysis of the volume of cavitation cloud in a cavitation tunnel using multiphase computational fluid dynamics simulations. *Scientific Journals of the Maritime University of Szczecin, Zeszyty Naukowe Politechniki Morskiej w Szczecinie* 76 (148), pp. 48–56, doi: 10.17402/585.
8. Jasionowski, R., Polkowski, W. & Zasada, D. (2018) Effect of crystalographic texture on cavitation wear resistance of as-cast CuZn10 alloy. *Archives of Metallurgy and Materials* 63 (2), pp. 935–940, doi:10.24425/122425.
9. Johnsen, E. & Colonius, T. (2009) Numerical simulations of non-spherical bubble collapse. *Journal of Fluid Mechanics* 629, pp. 231–262, doi: 10.1017/S0022112009006351.
10. Lauer, E., Hu, X.Y., Hickel, S. & Adams, N.A. (2012) Numerical modelling and investigation of symmetric and asymmetric cavitation bubble dynamics. *Computers & Fluids* 69, pp. 1–19, doi: 10.1016/j.compfluid.2012.07.020.
11. Lin, C., Zhao, Q., Zhao, X. & Yang, Y. (2018) Cavitation erosion of metallic materials. *International Journal of Georesources and Environment* 4 (1), pp. 1–8, doi: 10.15273/ijge.2018.01.001.
12. Liseikin, W D. (1999) *Grid Generation Methods*. Springer-Verlag.
13. Liu, H.L., Wang, J., Wang, Y., Zhang, H. & Huang, H. (2014) Influence of the empirical coefficients of cavitation model on predicting cavitating flow in the centrifugal pump. *International Journal of Naval Architecture and Ocean Engineering* 6 (1), pp. 119–131, doi: 10.2478/IJNAOE-2013-0167.
14. Müller, S., Helluy, P. & Ballmann, J. (2010) Numerical simulation of a single bubble by compressible two-phase fluids. *Numerical Methods in Fluids* 62 (6), pp. 591–631, doi: 10.1002/fld.2033.
15. Muttalli, R.S., Agrawal, S. & Warudkar, H. (2014) CFD simulation of centrifugal pump impeller using ANSYS-CFX. *International Journal of Innovative Research in Science Engineering and Technology* 03 (08), pp. 15553–15561, doi: 10.15680/ijirset.2014.0308066.
16. Naudé, C.F. & Ellis, A.T. (1961) On the mechanism of cavitation damage by nonhemispherical cavities collapsing in contact with a solid boundary. *Journal of Basic Engineering* 83 (4) pp. 648–656, doi: 10.1115/1.3662286.
17. Peyret, R. (1996) *Handbook of Computational Fluid Mechanics*. Academic Press.
18. Plesset, M.S. (1949) The dynamics of cavitation bubbles. *ASME Journal of Applied Mechanics* 16 (3), pp. 277–282, doi: 10.1115/1.4009975.
19. Plesset, M.S. & Chapman, R.B. (1971) Collapse of an initially spherical vapor cavity in the neighborhood of solid boundary. *Journal of Fluid Mechanics* 47 (2), pp. 283–290, doi: 10.1017/S0022112071001058.
20. Rasthofer, U., Wermelinger, F., Hadijdoukas, P. & Koumoutsakos, P. (2017) Large scale simulation of cloud cavitation collapse. *Procedia Computer Science* 108, pp. 1763–177, doi: 10.1016/j.procs.2017.05.158.
21. Sánchez Ocaña, W., Carvajal, C., Poalacín, J., Pazmiño, M.I., Jácome, E.S. & Basantes, L. (2018) Cavitation analysis with CFD techniques of the impeller of a centrifugal pump. *Indian Journal of Science and Technology* 11 (22), pp. 1–6, doi: 10.17485/ijst/2018/v11i20/123055.
22. Steller, J. & Gireń, B.G. (2015) *International cavitation erosion test. Final report*. Zeszyty Naukowe Instytutu Maszyn Przepływowych Polskiej Akademii Nauk w Gdańsku, Studia i Materiały, 560/1519/2015, doi: 10.13140/RG.2.1.4330.8883.
23. Szala, M. & Łukasik, D. (2016) Cavitation wear of pump impellers. *Journal of Technology and Exploitation in Mechanical Engineering* 2, pp. 40–44, doi: 10.35784/jteme.337.
24. Thompson, J.F., Warsi, Z.U.A. & Mastin, C.W. (1985) *Numerical Grid Generation*. Foundations and Applications, North Holland.
25. Tiwari, A., Pantano, C. & Freund, J.B. (2015) Growth-and-collapse dynamics of small bubble clusters near a wall. *Journal of Fluid Mechanics* 775, pp. 1–23, doi: 10.1017/jfm.2015.287.
26. Young, F.R. (1999) *Cavitation*. Imperial College Press, London.
27. Zakrzewska, D.E. & Krella, A.K. (2019) Cavitation erosion resistance influence of material properties. *Advances in Materials Science* 19 (4), pp. 18–34, doi: 10.2478/adms-2019-0019.
28. Zasada, D., Sienkiewicz, J.A. & Jasionowski, R. (2015) Grain size influences the corrosion and cavitation of Ni_3Al intermetallic alloys. *Metalurgija* 54, pp. 47–50.

Cite as: Jasionowski, R., Kostrzewa, W. (2024) Effect of mesh density and grid type on cavitation cloud volume. S*cientific Journals of the Maritime University of Szczecin, Zeszyty Naukowe Politechniki Morskiej w Szczecinie* 80 (152), 23–31.